

Bio-Optical Variability in Mayaguez Bay during the Rainy Season

Joel A. Quiñones Rivera, ja23_degrees@hotmail.com

Advisor: Fernando Gilbes

Abstract

Marine organisms in Mayagüez Bay are affected by chemical, biological and physical processes by changes in weather, topography and human activities. These processes induce fluctuations in salinity, turbidity, nutrient concentration, and biological productivity by suspending particles in the water that affects light penetration. This is critical for the bio-optical properties of the water that causes a direct effect on the photosynthetic organisms. This study used the data from different stations collected with an bio-optical rosette along the Mayagüez Bay and considering the Yagüez, Güanajibo and Añasco rivers during the rainy season. Our results show that large spatial variability of the bio-optical properties in Mayagüez Bay are generate by changes in rivers discharge. The new efforts finally show clear bio-optical evidence for land sea interactions. It also provides an important step for better application of remote sensing and validate the sensor AVIRIS.

Keywords: Mayagüez Bay, remote sensing, optical rosette, salinity, sediments, rivers, phytoplankton.

Introduction

Marine organisms in coastal areas are affected by chemical, biological and physical processes. These processes are caused by changes in weather, topography and human activities (agriculture, contaminants, urban development, and others). In the tropical coast, these changes produce certain differences and variations in the river discharge, which combines with the sediment eroded by urban development and agriculture, can accelerate the erosion of sediments. These processes induce fluctuations in salinity, turbidity, nutrient concentration, and biological productivity by suspending particles in the water that affects light penetration. This is critical for the bio-optical properties of the water that causes a direct effect on the photosynthetic organisms.

The western coast of Puerto Rico has spatial variations of phytoplankton and suspended sediments due to seasonal changes in rivers discharge. These sediments can be deposited on the shore or stay suspended in the water column affecting the dynamics of the phytoplankton communities.

The main rivers in the area are the Añasco, Yagüez and Güanajibo (Morelock et al., 1983). Agriculture is more abundance in the Añasco and Güanajibo Rivers basins. While in the Yagüez River basin, the urban development is predominant and contains more contaminants due to human activities. The proposed project was evaluate how these rivers affect the bio-optical properties of the water column in Mayagüez Bay by using historical field data. In this project I managed to:

- Develop the processing and analyses protocols for the collected data by using the software ArcGIS.

- Create a comprehensive database of the bio-optical properties of Mayagüez Bay.
- Determine the spatial variability (from inshore to offshore and through the water surface) of the bio-optical properties of Mayagüez Bay.
- Evaluate the effects of such variability in the phytoplankton growth.
- Provide recommendations for future validation of the hyperspectral sensor called AVIRIS.

Previous work

Several years ago a joint project with researchers from NASA-Stennis Space Center and the University of Puerto Rico at Mayagüez intended to use remote sensing for a better understanding of the land-sea interface in the west coast of Puerto Rico (Otero et al., 1994). However, the complexity of bay's optical properties and certain limitations of the technology at that time made it very difficult. Other studies have followed closely the problem of the continual discharges of sediments of the local rivers that affect the growing condition of the phytoplankton (Gilbes et al., 1996).

The river discharges appear to be the principal factor regulating the bio-optical properties of Mayagüez Bay, including the phytoplankton population. The effect of rivers discharge on the bio-optical properties of Mayagüez bay was more clearly recognized with the data recently collected by a custom-made bio-optical rosette (Figure 1). This rosette is made with several instruments that measure the different bio-optical properties of the water column.

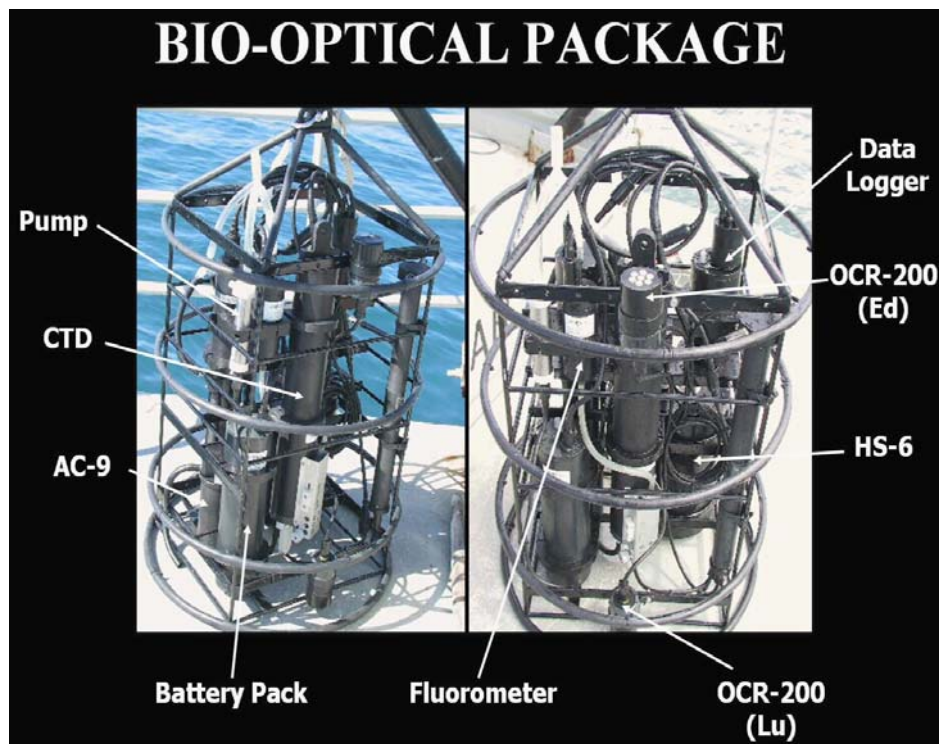


Figure 1: Customized rosette with different bio-optical instruments.

The west coast of Puerto Rico is now more developed and deforested. This causes higher erosion during the rainy season making it easier for the particles to be transported by the rivers. These suspended particles increase scattering and absorption, effectively attenuating light. But, these processes also increase nutrient concentration, promoting good condition for phytoplankton growth. This has been documented in a station closed to the sewage pipe, where nutrients are very high making it easier for phytoplankton growth (Gilbes et al., 1996). It was also observed that stations closed to the rivers mouth had higher concentrations of Chl-a because of the nutrient input, which are principal factors in the increase of Chl-a (Gilbes et al., 1996). Previous studies have proven the land-sea interactions in Mayagüez Bay. However, there are many processes that are not well understood. New samplings with new equipment are now providing the necessary data for a most comprehensive understanding of them. In this study I analyzed the collected data during the last sampling in the rainy season by using new GIS techniques (Arc-GIS, with 3D analysis). This work also intends to help with the validation of the sensor AVIRIS. This first step provides a better interpretation of the conditions affecting the phytoplankton and improves future remote sensing techniques in Mayagüez Bay.

Methodology

Field work

Field data was obtained during a cruise in Mayagüez Bay on August 19, of 2004. The sampling was performed during the wet season of the region and from inshore to offshore waters, covering the Añasco, Yagüez and Güanajibo Rivers, and the regions affected by the dumping of the sewage pipe. Table 1 shows the sampling stations.

Station	Latitude	Longitude
S01	18° 16.00'	67° 12.00'
S02	18° 16.00'	67° 13.10'
S04	18° 16.00'	67° 15.20'
S05	18° 14.40'	67° 11.40'
S07	18° 14.40'	67° 13.50'
S13	18° 12.20'	67° 09.78'
S15	18° 12.20'	67° 11.95'
S21	18° 10.25'	67° 11.10'
S23	18° 10.25'	67° 13.15'
S24	18° 10.25'	67° 14.80'

Table 1: Latitude and longitude of sampled stations.

Ten (10) stations were sampled with the optical package (Figure 2). Coastal areas have large spatial variability of bio-optical properties. This state-of-art methodology allows measuring this variability more efficient and accurate because all the instruments are collecting profiles of data at the same time and from the same water parcel. The bio-optical rosette is made of several profiling instruments.

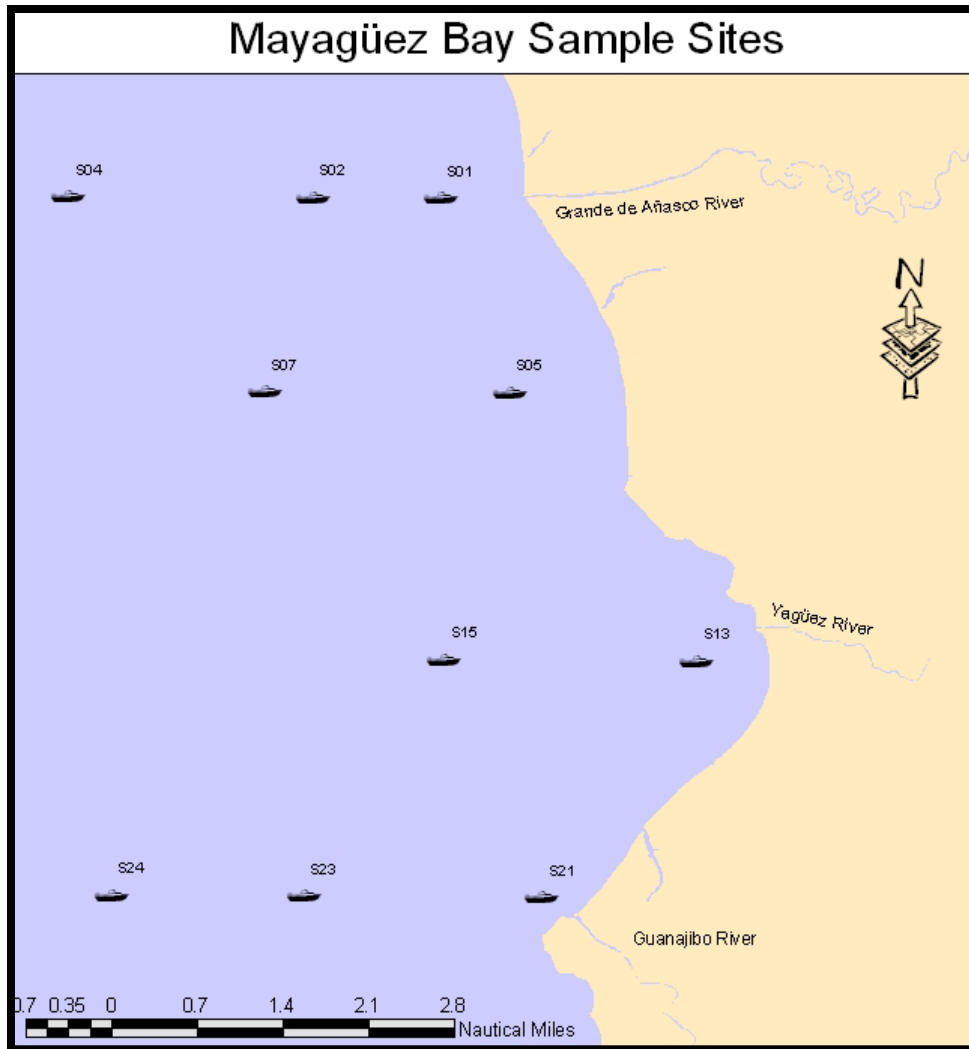


Figure 2: Study area showing the ten sampled stations.

A CTD (Seabird SBE-19 with pump) measured temperature and salinity. A small fluorometer (Model Wet Star from Wet Labs) measured chlorophyll fluorescence. The spectral transmittance, $c(\lambda)$, and spectral adsorption, $a(\lambda)$, was measured over nine wavelengths with the AC-9 meter (from Wet Labs). The backscattering coefficient, $b_b(\lambda)$, at six wavelengths was measured with the HydroScat-6 (from Hobi Labs). Upwelling radiance, $L_u(0^-, \lambda)$, and downwelling irradiance, $E_d(0^-, \lambda)$, was obtained using a submersible radiometer (Model OCR-200 from Satlantic).

The optical measurements from the profilers were compared with water samples measurements collected at two depths. Concentration of phytoplankton chlorophyll-a was obtained using the standard fluorometric method (Yentsch and Menzel, 1963). Optical absorption spectra of the colored dissolved organic matter, $a_g(\lambda)$, was determined with Perkin Elmer double-beam spectrophotometer following the method described by Bricaud et al. (1981). Concentrations of suspended sediments were determined using the standard weight difference method.

Instrument	Company	Parameter
CTD SBE-19	Seabird	Depth, Temperature, Salinity
WetStar	Wet Labs	Chlorophyll Fluorescence
Spectral Transmittance and Absortion	Wet Labs	Nine wavelengths with the Ac- 9+
HydroScat-6 sensor	Hobi Labs	Backscattering coefficient six wavelengths
OCR-507	SatLantic	Upwelling Radiance and Downwelling Irradiance

Table 2: Information about the instrument of the bio-optical rosette.

Lab work

The data collected with the bio-optical rosette was initially:

- The data were processed and organized with the Microsoft Excel software.
- All noisy data from each instrument were removed in the 10 stations and only the downcast was be used for further analyses.
- Since the instruments measure continuously every second during the deployment, it was necessary to merge the data and make median calculations in order to eliminate the noise for each parameter (appendix 1).
- After the complete database was developed in Excel it was necessary saved the data in DBase IV in order to import the file to ArcGIS.
- For using the latitude and longitude of the 10 stations correctly to ArcGIS, it was required to use the software Corspron 6 using geographic location of Puerto Rico. This software changes the grades to decimal numbers that ArcGIS can process and generated a map with the real position of the stations. All these data was imported to ArcGIS for new visualization techniques, including thematic maps and 3D analyses of the bio-optical parameters.
- Contour lines, stations positions, legend to observe changes in the parameters in each map were made with the 3D analyses and properties in the ArcGIS.
- Once the GIS database was created a comprehensive analysis was made using the surface data of the 10 stations.
- A correlation analysis was made to establish the relationship between them.
- I was focused on the analysis of salinity, fluorescence and backscattering of suspended particles in different wavelengths. This helped to establish the land-sea interactions.
- Finally a thematic map was created to explain the processes.

Results

The following images were the results of a long time effort.

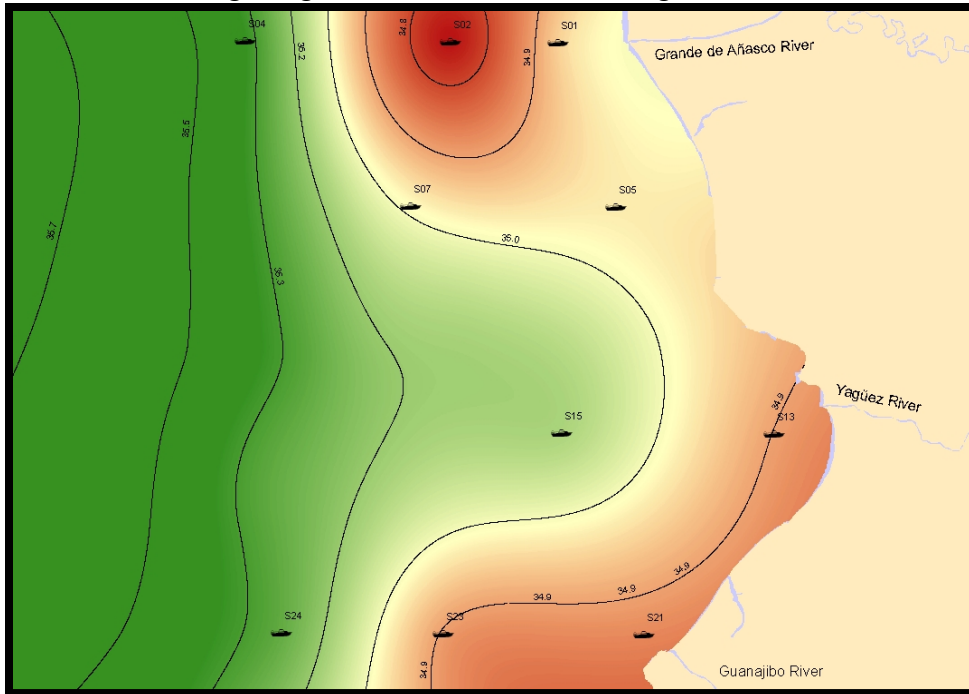


Figure 3a: Salinity (green color) was affected by the fresh water (red color) that comes from the rivers along the Mayagüez bay.

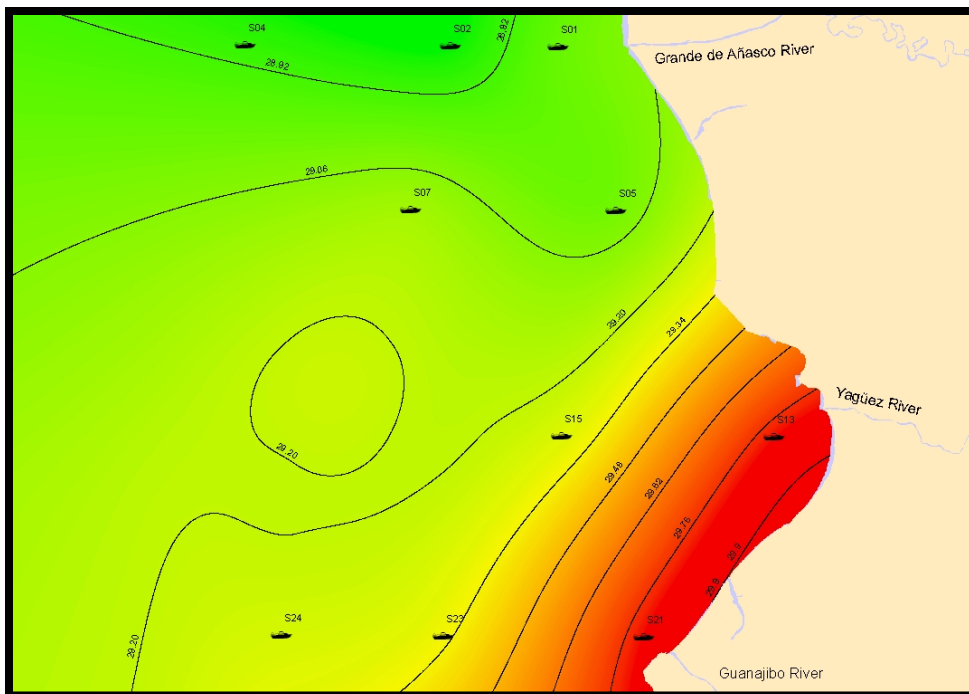


Figure 3b: Show that the higher temperature (dark color) comes from Yagüez and Güanajibo area than Añasco area although is approximately 1 grades of difference.

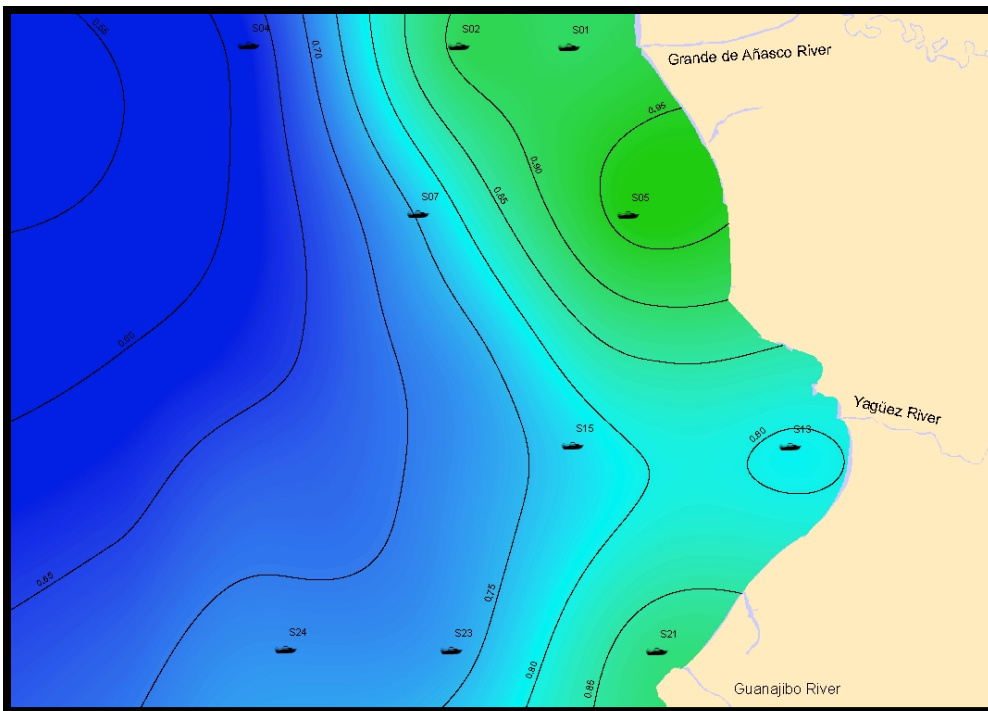


Figure 3c: Show a growth of phytoplankton population in Añasco and Güanajibo area in the rainy season, it observes the fluorescence (green color) product of chlorophyll-a.

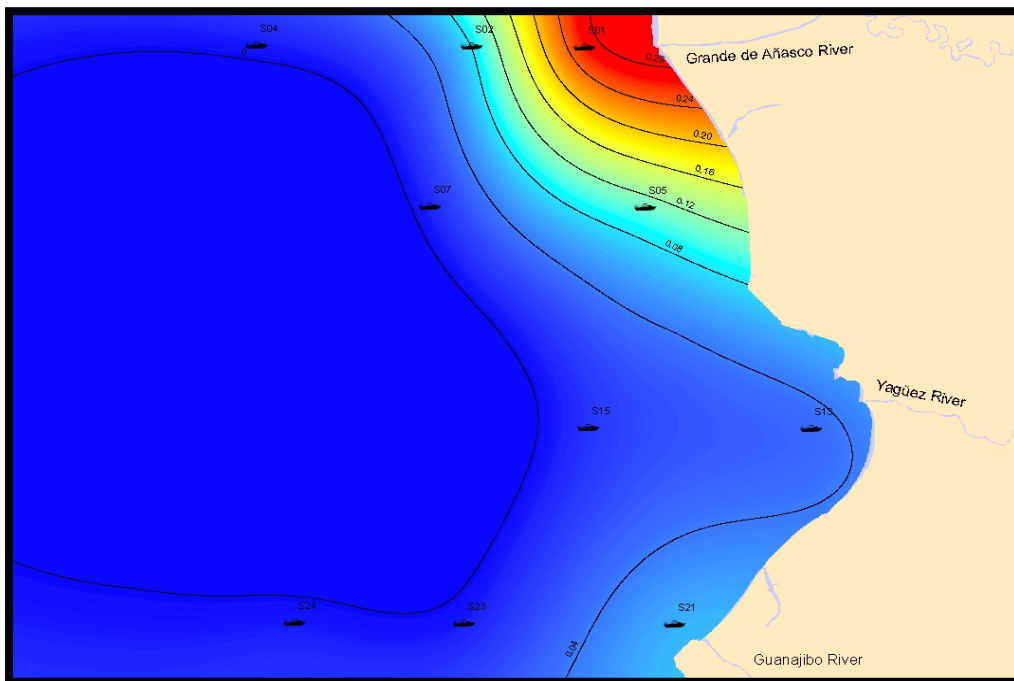


Figure 3d: Show higher values of backscattering (wavelength 589) in the Añasco area by the high concentration of sediments that load the Añasco river in the rainy season.

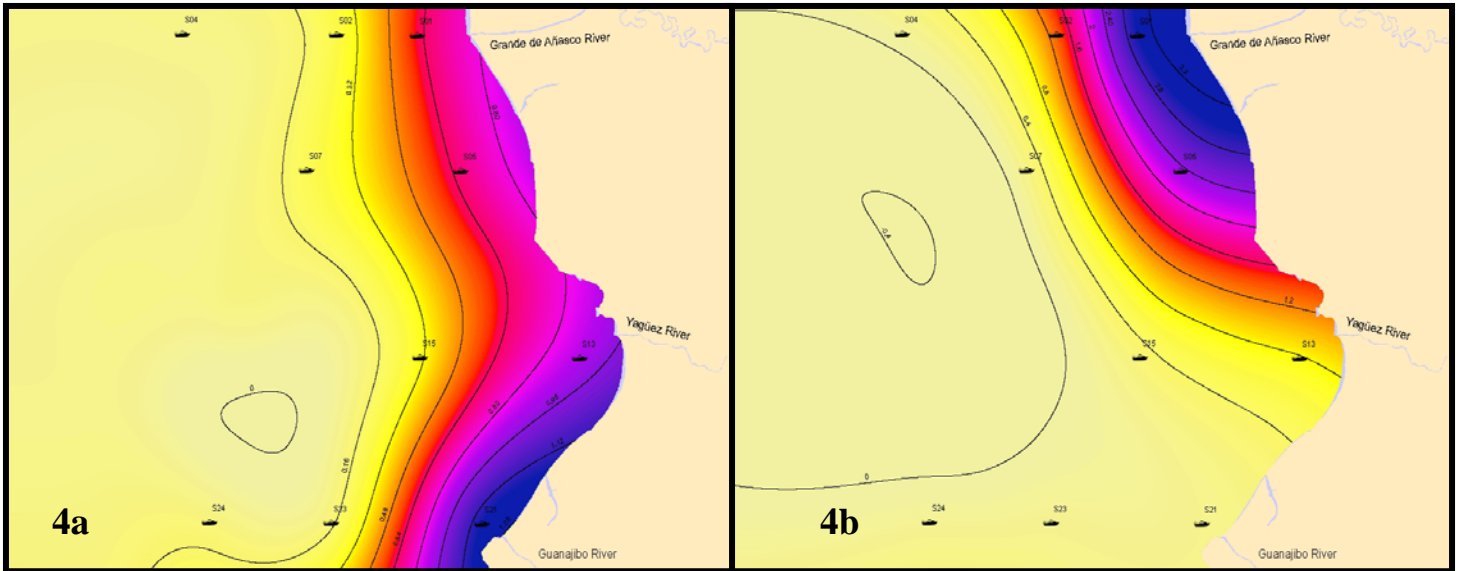


Figure 4a: Show the absorption at 1 meter of depth. Figure 4b: Show the absorption at 0.5 meter of depth (Both with wavelength 412).

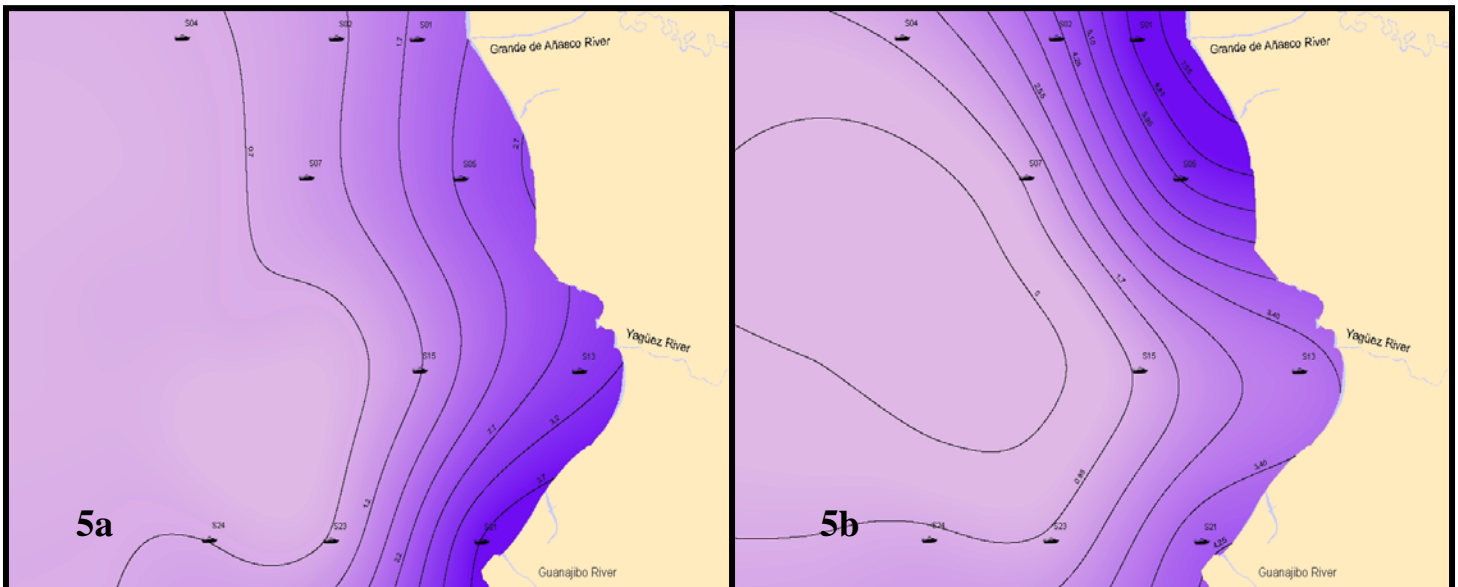


Figure 5a. Show the attenuation at 1meter of depth. Figure 5b: Show the attenuation at 0.5 meter of depth (Both with wavelength 412).

Discussion

Mayagüez Bay is a highly dynamic environment that shows large spatial variability of bio-optical properties. To the collected data demonstrated how these parameters changes due to the high river discharge during the rainy season. The Añasco River has the largest basin on the west coast, and drained more material than the Yagüez and Güanajibo Rivers during the wet season. The Añasco River discharges high amount of sediments, this may indicate a high concentration of nutrients in the environment,

supporting in turn optimum conditions for phytoplankton growth. During the wet season, the northern stations of the bay show the higher concentration of Cl-a. Closest to the rivers mouth especially in Güanajibo and Añasco Rivers, it shows higher concentrations of Cl-a that produces high fluorescence, a raw estimate of phytoplankton biomass. (Figure 3c).

In the Güanajibo River we can observe an increment of fluorescence but it is lower than in the Añasco River. In Yagüez River this concentration is low because this river discharges less sediment and nutrient (due to the urbanization) during the rainy season and the phytoplankton is less. A positive correlation between Cl-a and the suspended sediments was shown, where there was an inshore-offshore decrease in both parameters.

Other parameter that was affected by the discharge of the rivers was the salinity (Figure 3a). It can observe that Añasco and Güanajibo Rivers transport more fresh water than the Yagüez River.

However, lenses of low salinity were related with high optical properties (absorption, attenuation and backscattering) at the surface of the water along the inshore of Mayagüez Bay. Backscattering in all different wavelengths was higher in the Añasco River than in Güanajibo and Yagüez rivers, because this river transports higher concentrations of sediments to the coast during the rainy season (appendix 3).

The AVIRIS image collected during the same day of the field sampling showed that the plume formed in the surface of Añasco River was higher than those in the Yagüez and Güanajibo Rivers (Figure 6). However, our analyses shown differences in the optical properties between 1.0 and 0.5 meter (appendix 2-4). At 0.5 meter, both parameter (absorption and attenuation) were higher due to the plumes that was formed during that day (Figure 4b, 5b).

Temperature maps were created to analyze the changes in temperatures along the Mayagüez Bay (Figure 3b), but only 1°C was the difference between the north and south part of the bay. In Añasco coast the temperature was 28.8 °C and in Yagüez and Güanajibo coast the temperature was 29.1°C. A possible reason for these temperature differences is that the south part of the bay is shallower and it can get warmer than the north part.



Figure 6: Study area in Mayagüez Bay as detected by the AVIRIS sensor.

Conclusions

River discharge appears to be the principal factor regulating the bio-optical properties in Mayagüez Bay, including the phytoplankton populations, during the rainy season. The western basin of Puerto Rico is highly developed and deforested, which favors erosion and transference of soil particles into the river water. These suspended particles cause turbidities in the water and increase scattering and absorption, effectively attenuating light. But it also increase the nutrients concentrations that help phytoplankton

growing. During the wet season, the Añasco River shows the higher dynamics and it is very important for phytoplankton due to the amount of nutrients that arrive to the coast.

The results of this project, were very important for future validation of the sensor AVIRIS. These current efforts will improve future techniques of remote sensing in this region. Also for future works, I recommend tutorials of 3D analysis of the ArcGIS program with anticipation, in order to take advantage of the time correctly and to familiarize with the project.

Acknowledgements

I want to thanks to Fernando Gilbes to provide me the data required to make this project, and Ruben Raimundí to support me and teach me how to use the program ArcGIS. This project was founded by NOAA-CREST.

References

- Bricaud, A., Morel, A., and Prieur, L., 1981, Absorption by dissolved organic matter of the sea (yellow substance) in UV and visible domains: *Limnology and Oceanography*, v. 26, p. 43-53.
- Gilbes, F., López, J.M., and Yoshioka, P.M., 1996, Spatial and temporal variations of phytoplankton chlorophyll-a and suspended particulate matter in Mayagüez Bay, Puerto Rico: *Journal of Plankton Research*, v. 18, p.29-43.
- Miller, R.L., Cruise, J.F., Otero, E., and Lopez, J.M., 1994, Monitoring suspended particulate matter in Puerto Rico: field measurements and remote sensing: *Water Resources Bulletin*, v. 30, p. 272-283.
- Morelock, J., Grove, K., and Hernandez, M.L., 1983, Oceanography and patterns of shelf sediments Mayaguez, Puerto Rico: *Journal of Sedimentary Petrology*, v. 53, p. 371-381.
- Yentsch, C., and Menzel, D., 1963, A method for the determination of phytoplankton chlorophyll and phaeophytin by fluorescence: *Deep-Sea Research*, v. 10, p. 221- 231.

Appendix 1

Show all clear and final data (backscattering (bb), attenuation (c), absorption (a), temperature, salinity and fluorescence) that was used to import to ArcGIS to generate maps.

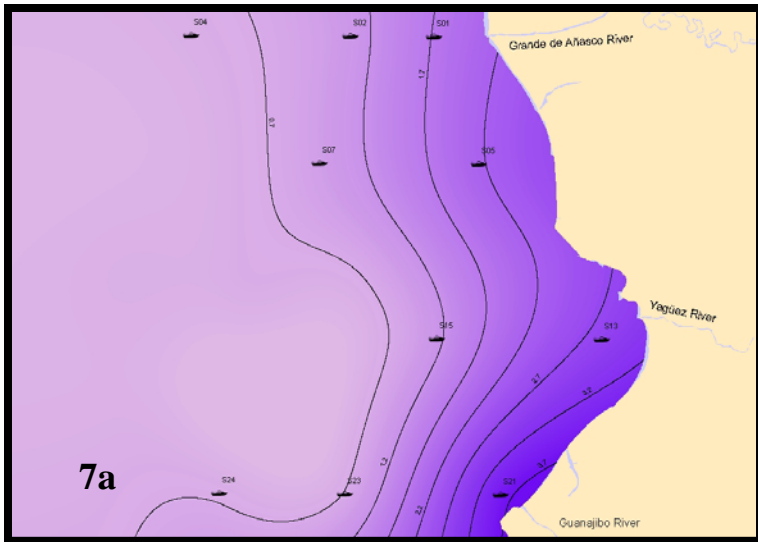
Station	Latitude	Longitude	Salinity	Temperature	Fluorescence
S01	118929.8	248131.5	34.9681	28.99085	0.90475
S02	116991.2	248139.7	34.684	28.8572	0.9109
S04	113290.2	248156	35.384	28.9009	0.6215
S05	119975	245175.6	35.0071	29.0194	0.9634
S07	116273.5	245191.3	35.0331	29.1259	0.7546
S13	122814.4	241105.7	34.8969	29.8015	0.7949
S15	118988.6	241121.3	35.1654	29.2713	0.7741
S21	120472.4	237518	34.8582	29.807	0.8779
S23	116857.5	237533.2	34.89265	29.3254	0.73385
S24	113948	237545.9	35.2965	29.2464	0.71855

Station	a412	a440	a488	a510	a532	a555	a650	a676	a715
S01	0.61785	0.553505	0.44058	0.408685	0.35919	0.32472	0.269835	0.29016	0.232145
S02	0.23646	0.21545	0.19108	0.17072	0.14165	0.13143	0.09994	0.12046	0.09635
S04	0.09481	0.08961	0.06907	0.06746	0.05339	0.05008	0.03539	0.04293	0.04021
S05	0.66904	0.58767	0.46941	0.43432	0.38385	0.35104	0.28151	0.30334	0.24787
S07	0.20658	0.18847	0.14655	0.13396	0.11162	0.10237	0.0751	0.09253	0.07359
S13	0.89329	0.78057	0.62054	0.5628	0.501315	0.45738	0.35967	0.38884	0.32908
S15	0.3052	0.28036	0.21761	0.19639	0.16911	0.15292	0.11921	0.14497	0.1089
S21	1.1809	1.04323	0.83613	0.77205	0.69591	0.63998	0.51659	0.55826	0.46644
S23	0.1463	0.13721	0.105115	0.10121	0.079905	0.07073	0.0521	0.072635	0.05274
S24	0.12496	0.11602	0.088785	0.0864	0.066485	0.060775	0.0428	0.06223	0.04643

Station	c412	c440	c488	c510	c532	c555	c650	c676	c715
S01	1.81131	1.72892	1.62256	1.5688	1.52416	1.48329	1.329415	1.288775	1.28003
S02	1.1171	1.0592	0.95507	1.05656	1.03655	0.98914	0.8841	0.8558	0.86225
S04	0.61344	0.59705	0.55268	0.53381	0.50874	0.50195	0.44638	0.43278	0.44319
S05	2.27005	2.15397	2.012845	1.95555	1.899735	1.852915	1.69563	1.626295	1.63374
S07	0.96968	0.91983	0.85846	0.82656	0.80305	0.77609	0.70645	0.68235	0.69093
S13	2.95896	2.82837	2.62778	2.55493	2.475255	2.41062	2.20812	2.156545	2.08997
S15	1.18522	1.13122	1.06244	1.01543	0.98758	0.96689	0.87972	0.86289	0.85642
S21	3.73614	3.56279	3.35129	3.25787	3.19332	3.11644	2.87774	2.80454	2.78239
S23	0.76234	0.72662	0.67749	0.652835	0.63589	0.61833	0.56367	0.54579	0.56012
S24	0.6894	0.661985	0.61682	0.59345	0.57093	0.56174	0.50851	0.49669	0.5084

Station	bb442	bb470	bb510	bb589	bb620	bb671
S01	0.130366	0.136165	0.163557	0.265134	0.135984	0.209596
S02	0.069955	0.064003	0.069089	0.081868	0.078265	0.081044
S04	0.007306	0.00575	0.005052	0.004415	0.003987	0.004188
S05	0.124303	0.112535	0.111097	0.106982	0.100171	0.106396
S07	0.012608	0.010384	0.009212	0.007816	0.00741	0.007886
S13	0.042072	0.037785	0.03569	0.033906	0.03123	0.031743
S15	0.017333	0.015088	0.014327	0.012603	0.01157	0.012047
S21	0.067563	0.061497	0.061038	0.060273	0.056248	0.057253
S23	0.009018	0.006861	0.006059	0.005352	0.00493	0.005179
S24	0.007605	0.005421	0.005309	0.004504	0.004212	0.004409

Appendix 2



Appendix 3

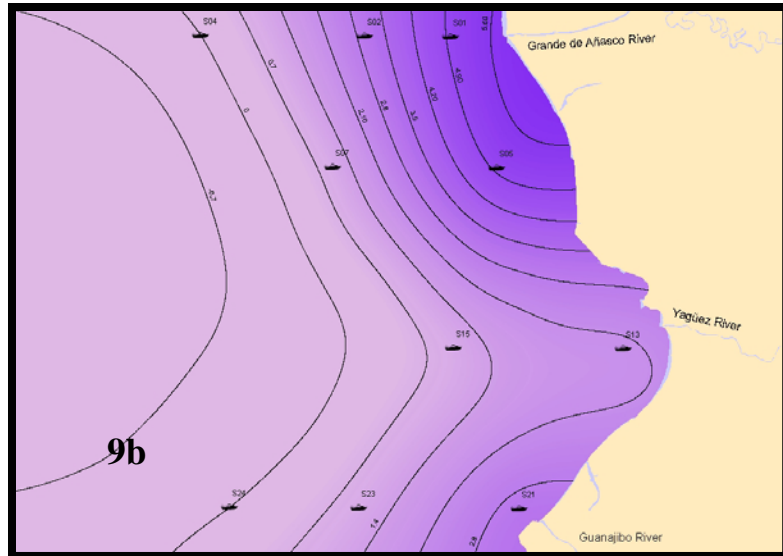
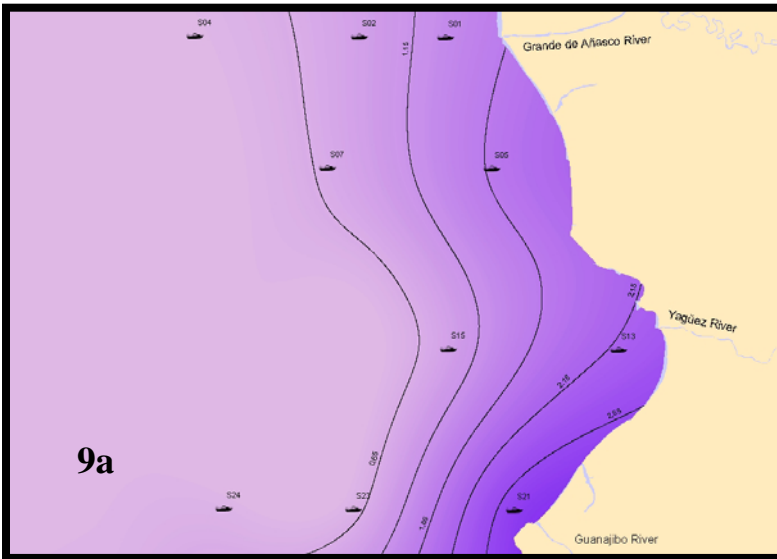


Figure 9a: Show the attenuation at 1 meter of depth. Figure 9b: Show the attenuation at 0.5 meter of depth. (Wavelength of 650).

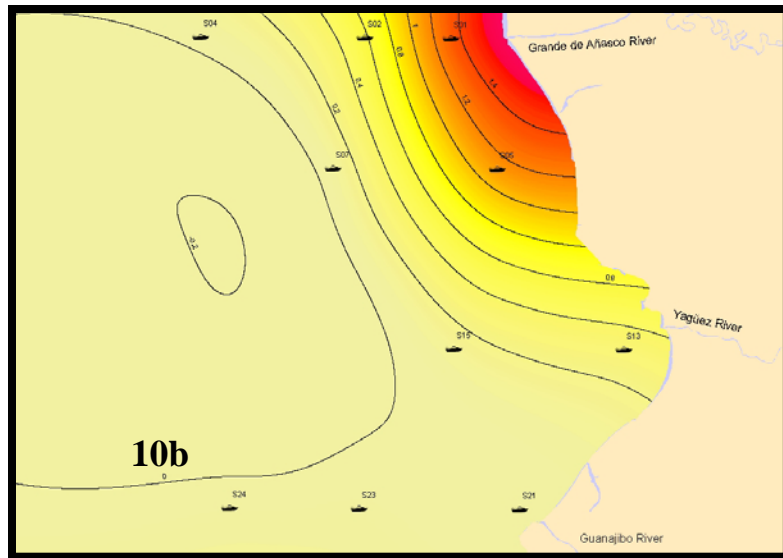
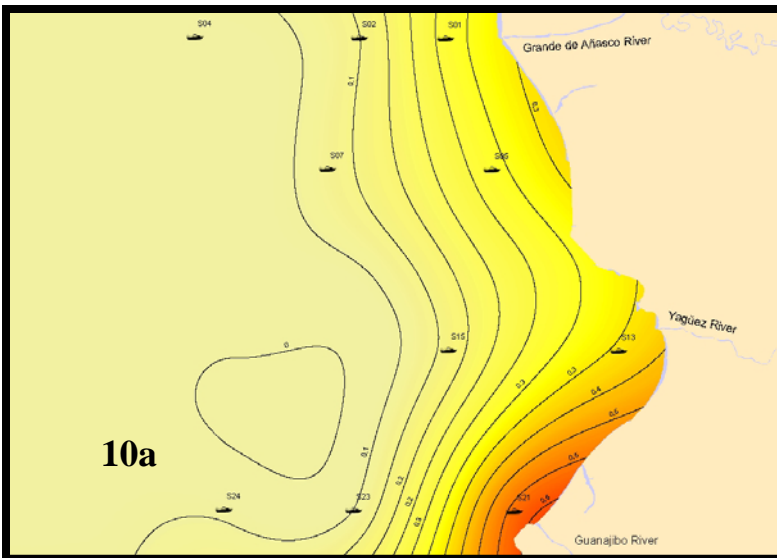


Figure 10a: Show the absorption at 1 meter of depth. Figure 10b: Show the absorption at 0.5 meter of depth (Both with wavelength 650).

Appendix 4

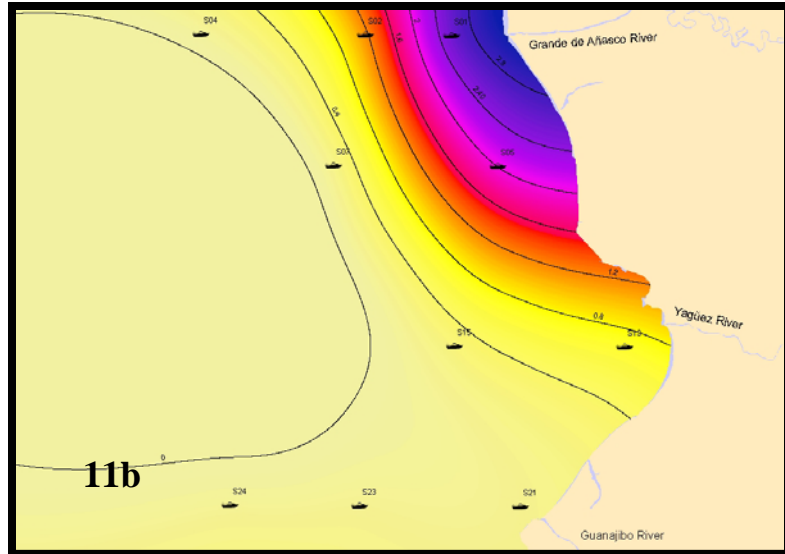
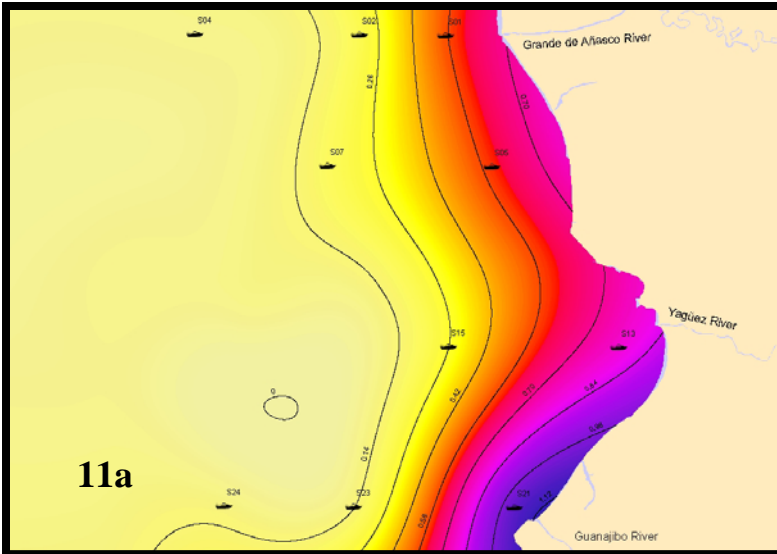


Figure 11a: Show the absorption at 1 meter of depth. Figure 11b: Show the absorption at 0.5 meter of depth (Both with wavelength 440).

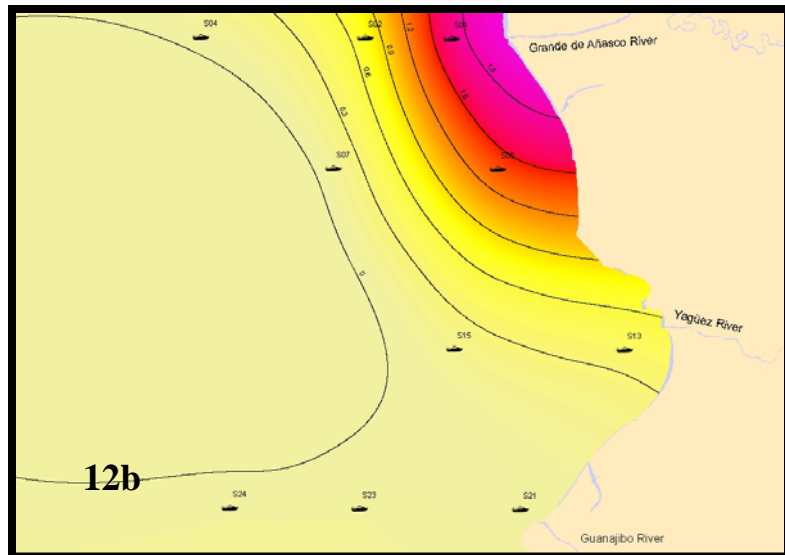
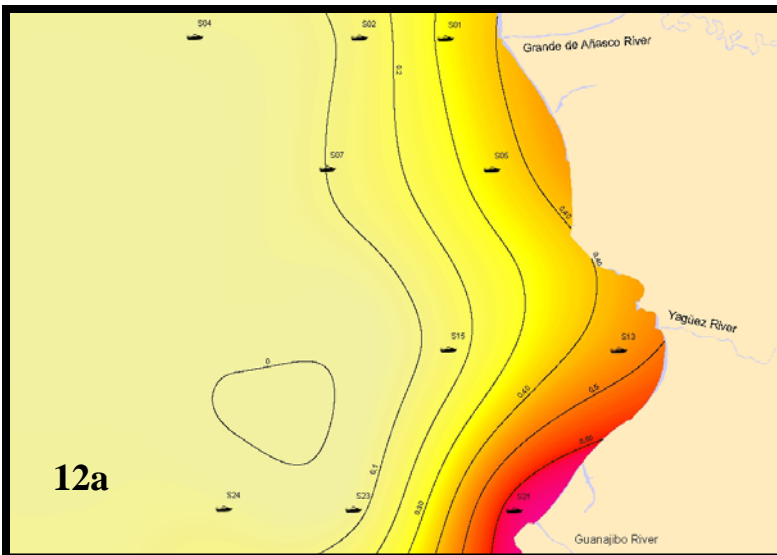


Figure 12a: Show the absorption at 1 meter of depth. Figure 12b: Show the absorption at 0.5 meter of depth (Both with wavelength 555).

Appendix 5

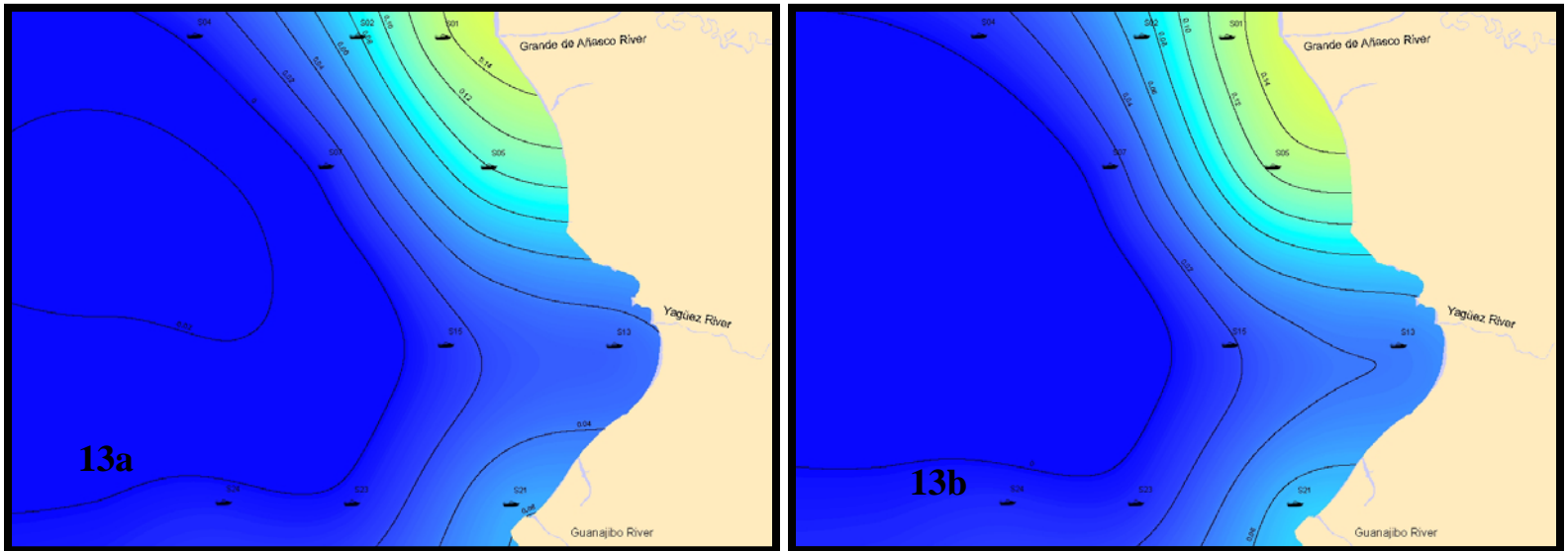


Figure 13a: Show the backscattering (wavelength 442). Figure 13b: Show the backscattering (wavelength 620).